

## **GPR RESEARCH IN WOJANÓW RAILWAY TUNNEL, SUDETES MTS., POLAND**

ADAM SZYNKIEWICZ

KART-GEO, WROCLAW, POLAND, ADAM.SZYNKIEWICZ@GMAIL.COM

### **ABSTRACT**

*In the area of Wojanów railway tunnel (Sudetes Mts., Poland), Ground Penetrating Radar (GPR) was employed in the context of a geotechnical research for the purposes of designing the tunnel renovation. Various antennas were used, with 100 MHz, 250 MHz, and 800 MHz central frequencies. The sections recorded above the tunnel with 100 MHz antennas allowed estimating at what distance from the tunnel casing, behind the housing, there is a solid rock. The cross-sections recorded with 250 MHz antennas allowed figuring out the structure of the ground behind the tunnel casing. The analysis of data obtained with 800 MHz antennas made it possible to precisely determine the condition of the tunnel casing and of the casing reinforcement zone. An attempt was also made to analyse GPR data in a three-dimensional system, to study the general state of the ground behind the tunnel casing; the analysis indicated loosening rocks and empty spaces behind the tunnel casing.*

**KEYWORDS:** Ground Penetrating Radar (GPR); Civil engineering; Railway tunnel.

### **1. INTRODUCTION**

Ground-penetrating radar (GPR) is a safe and valuable method for the non-destructive testing of transport infrastructures, including tunnels [1], [2]. In the scientific literature, several works address the successful use of GPR for the assessment of roads and bridges, whereas a rather limited number of case studies deal with the use of this technique for the investigation of tunnels [3]–[23]. This is probably due to the fact that tunnel inspections present considerable practical difficulties, compared to roads and bridges, therefore they are less frequent. The objectives of this paper are to present the results of a GPR survey carried out in Wojanów railway tunnel, in Poland, and to provide practical guidelines for GPR inspection of tunnels.



## Location of Wojanów railway tunnel

Wojanów railway tunnel is located in the Sudetes Mts., in the south west of Poland, about 15 km east of Jelenia Góra.

The tunnel is carved in granite and is located at an altitude of about 376 m above sea level, about 30 m below the ridge of the tunnel mountain and about 20 m above the water level in the Bóbr river. The water level in the Bóbr river is at an average height of about 356 m above sea level.

Wojanów railway tunnel was built in 1867. The length of the tunnel is 293.15 m, the vertical height is 6.82–7.22 m, and the maximum horizontal width of the tunnel is 7.09–7.38 m. The walls of the tunnel are enclosed with granite blocks, which dimensions are: 1–0.35 m × 0.4–0.6 m. The granite housing blocks have a weight of 600–1200 kg. Eastern and Western tunnel entrances (E and W inlet to the tunnel) are enclosed with stone portals made of granite blocks.

After 150 years of operation and progressing degradation, this tunnel requires renovation and protection. In the tunnel housing there are numerous cracks and displacements of the rock blocks of the casing. In the ceiling of the tunnel there are numerous gaps between the housing blocks. Recently, wooden wedges have been torn into these gaps to prevent block housing from falling out. On the ceiling and side walls there are numerous places of slow water outflow and precipitation of calcium carbonate ( $\text{CaCO}_3$  speleothems). In the eastern part of the tunnel, water flows out from the gaps between the housing blocks in the form of a stream.

## Geological situation

Wojanów railway tunnel was forged in granite rocks of the Upper Carboniferous [24]–[26]. This granite is coarse-grained, cracked and cut with quartz veins and veins of aplite. There are cracks in the granite, inclined towards the south. In the south-eastern part of the tunnel mountain, there is an old mining tunnel (about 200 m long) where vertical veins of quartz and aplite, running NE–SW, have been found. In the outcrops, occurring near the western outlet of the tunnel, dislocations of rocks in direction NW–SE and discharges towards the south were observed.

## Horizontal geological drilling in the tunnel

In the walls of Wojanów tunnel, fifteen horizontal geological drillings were drilled to a depth of 2–4 m (Figure 1). Nine holes were made in the northern wall of the tunnel (from the T1 side) and six in the southern wall of the tunnel (from the T2 side). Geological drilling holes (indicated by “otw.” in Figure 1) were made in the walls at a height of 1, 2, and 3 m above the floor (for borehole locations, see also Figure 2). The drilling shows that the granite blocks of the tunnel casing have a thickness of 30–55 cm. Behind the housing there is a strengthening zone (concrete, cement), which has a thickness up to 1.1 m (in some places up to 2 m). From 0.7 to 4.5 m there are granite debris, gravels and sands. Behind the casing of the tunnel, at a distance of 2–4 m, there is weathered granite, heavily cracked granite, or hard granite with rare cracks.

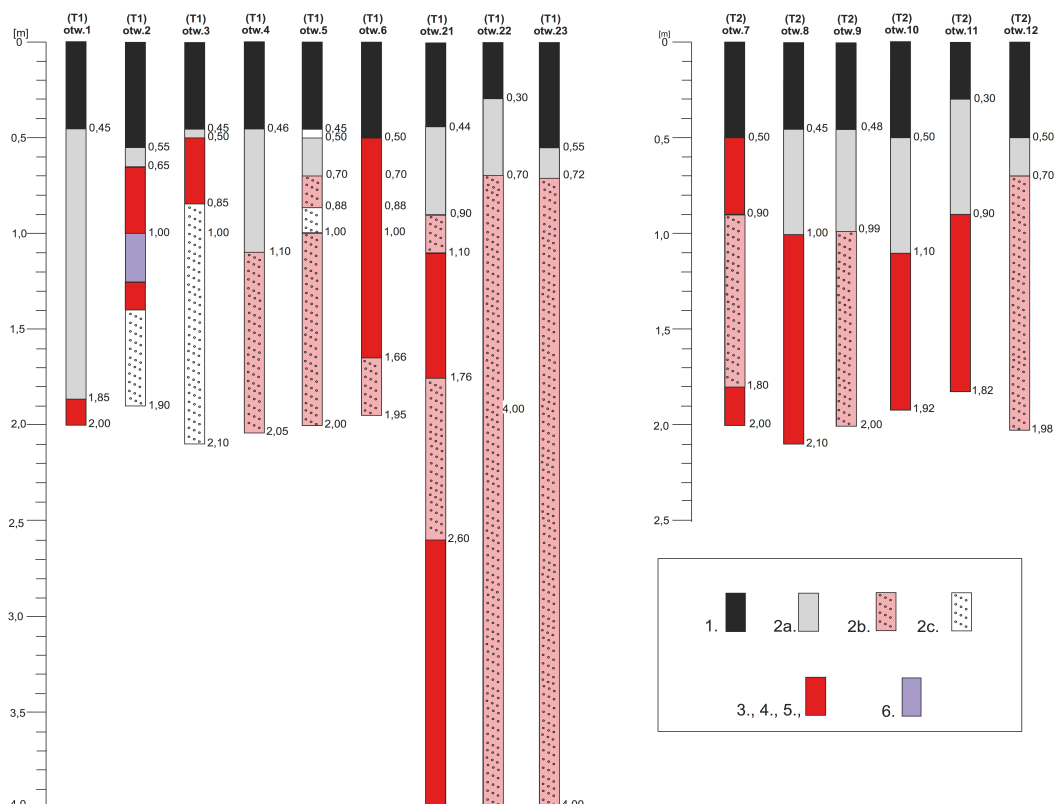


**FIG. 1** – Lithology information about Wojanów tunnel, obtained by drilling its walls. Legend: 1 – housing made of granite rock block; 2a – concrete, cementation zone; 2b – granite weathering (gravel) plus granite fragments; 2c – gravel and sand; 3 – weathered granite; 4 – granite strongly cracked; 5 – solid granite (rare cracks); 6 – aplit.

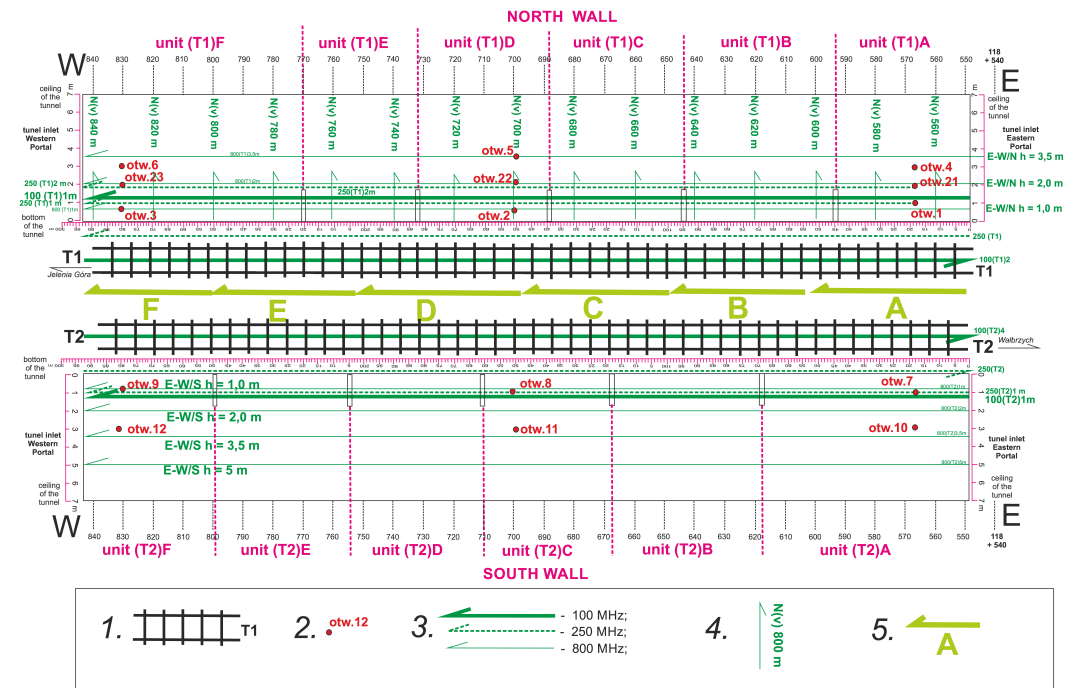


**FIG. 2** – Scheme illustrating the GPR cross-section and borehole locations in Wojanów tunnel. Legend: 1) Tracks; 2) Horizontal boreholes; 3) Horizontal GPR cross-sections; 4) Vertical GPR cross-sections on the northern wall (800 MHz antenna); 5) GPR cross-section on the ceiling (800 MHz antenna).

### Water in the area of the tunnel

The scheme of basic hydraulic properties for areas of occurrence of crystalline rocks [27] was used to visualize groundwater in the area of the tunnel. There are three aquifers (see Figure 3):

- Zone I - A weathering cover with variable thickness, high water capacity and low water conductivity. This is the zone that affects most the eastern and western inlets of the tunnel.
- Zone II - A densely fractured rock mass with high conductivity and low capacity.
- Zone III - A zone of deep circulatory pathways, which includes cracks accompanying fault zones, with the lowest capacity and hydraulic conductivity.

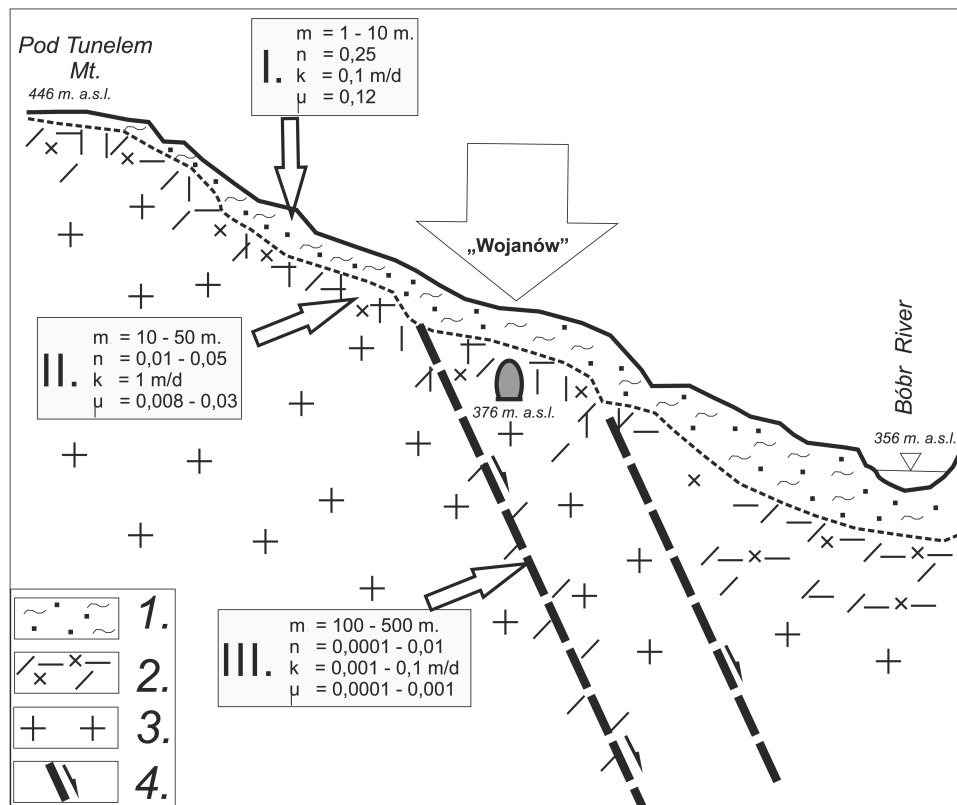


**FIG. 3** – Occurrence of groundwater in Wojanów tunnel region, in areas of igneous and metamorphic rocks with low porosity but relatively high fissures, with reference to the geological and topographic situation of the tunnel. Legend: 1) Weathering cover; 2) Weathered and strongly cracked granite; 3) Cracked granite; 4) Fault zone. Symbols: m - thickness of the wet zone, n - effective porosity, k - filtration coefficient,  $\mu$  - gravitational drainage.

## 2. METHODOLOGY OF GPR RESEARCH

### GPR data collection

GPR research was carried out for the purposes of designing the tunnel renovation. To facilitate the description of research results and the identification of rock mass variability occurring behind the housing, the entire length of the tunnel (from the eastern portal towards the western portal) was divided into sections denominated as follows: from (T1)A to (T1)F and from (T2)A to (T2)F (see again Figure 2; note that the kilometers of the railway route are also reported in the scheme).

GPR measurements were carried out at night, when there was no train movement and it was possible to switch off the electricity in the

electric traction. To work at the tunnel ceiling, a train was used which is normally employed to repair the electric traction. All tests were made with antennas facing the tunnel walls (Figure 4). Shielded antennas were used, with three central frequencies: 100, 250, and 800 MHz.

The following cross-sections were recorded with the use of 100 MHz antennas: over the tunnel, along the walls of the tunnel at a height of 1 m, and on the bottom of the tunnel (between the rails of railway tracks). The following cross-sections were recorded with the use of 250 MHz antennas: along the walls of the tunnel, at heights of 1 meter and 2 meter, along the tunnel bottom and along the base of the walls of the tunnel casing. Finally, cross-sections with the use of 800 MHz antennas were recorded along the tunnel walls, at heights of 1, 2, 3.5, and 5 m, as well as along the ceiling of the tunnel (see Figures 2 and 5).

### **Methodology for GPR data interpretation**

Various color palettes and customary filter combinations were used to analyze GPR data. In Figure 6, an example of processed radargram is presented; this is a fragment of a cross-section recorded with 800 MHz antennas along the north wall, at 1 m height (the (T1) 800\_1m cross-section). By using suitable filters, it was possible to improve the visualization of the gaps in the tunnel casing (radargram A in Figure 6) and of the housing blocks (part B in Figure 6). The calibration of the GPR radargram depth scale was made on the basis of drilling (Figure 7).

After selecting the color palette, applying filters, calibrating the depth scale, and obtaining a more readable image of the GPR data, the geological interpretation started. On the various GPR sections, the following lithological assemblies were distinguished: housing made of granite rock blocks; concrete and cementation zone; granite weathering (gravel) with granite fragments; weathered granite; strongly cracked granite; solid granite with rare cracks. An example is presented in Figure 8, where the following features are also shown: control points; niches in the tunnel walls; locations of drilling holes; housing border (housing blocks); boundary of cementing/concreting zone; boundaries between housing blocks together with cementation and clastic pieces behind the housing; boundary between mashing (weathered) and cracked, weathered granite rocks; detected anomalies. This approach was applied to all GPR cross-sections and a series of images were created.



**FIG. 4** – GPR research in Wojanów tunnel: 800 MHz antennas directed towards the ceiling of the tunnel housing.

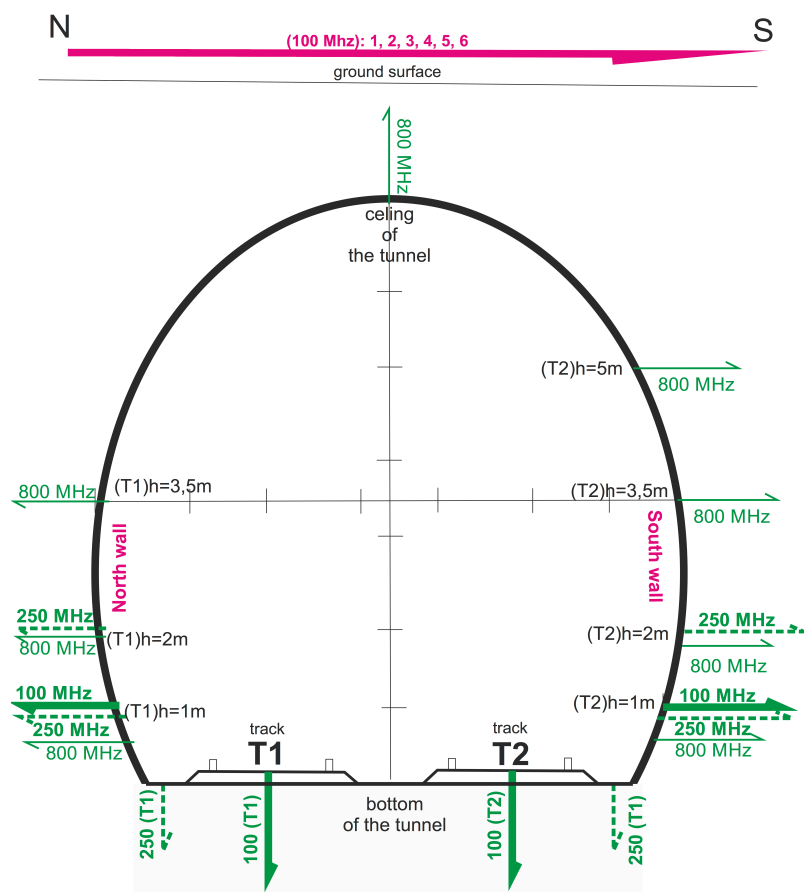


**FIG. 5** – Location of GPR sections in Wojanów tunnel (schematic sketch).



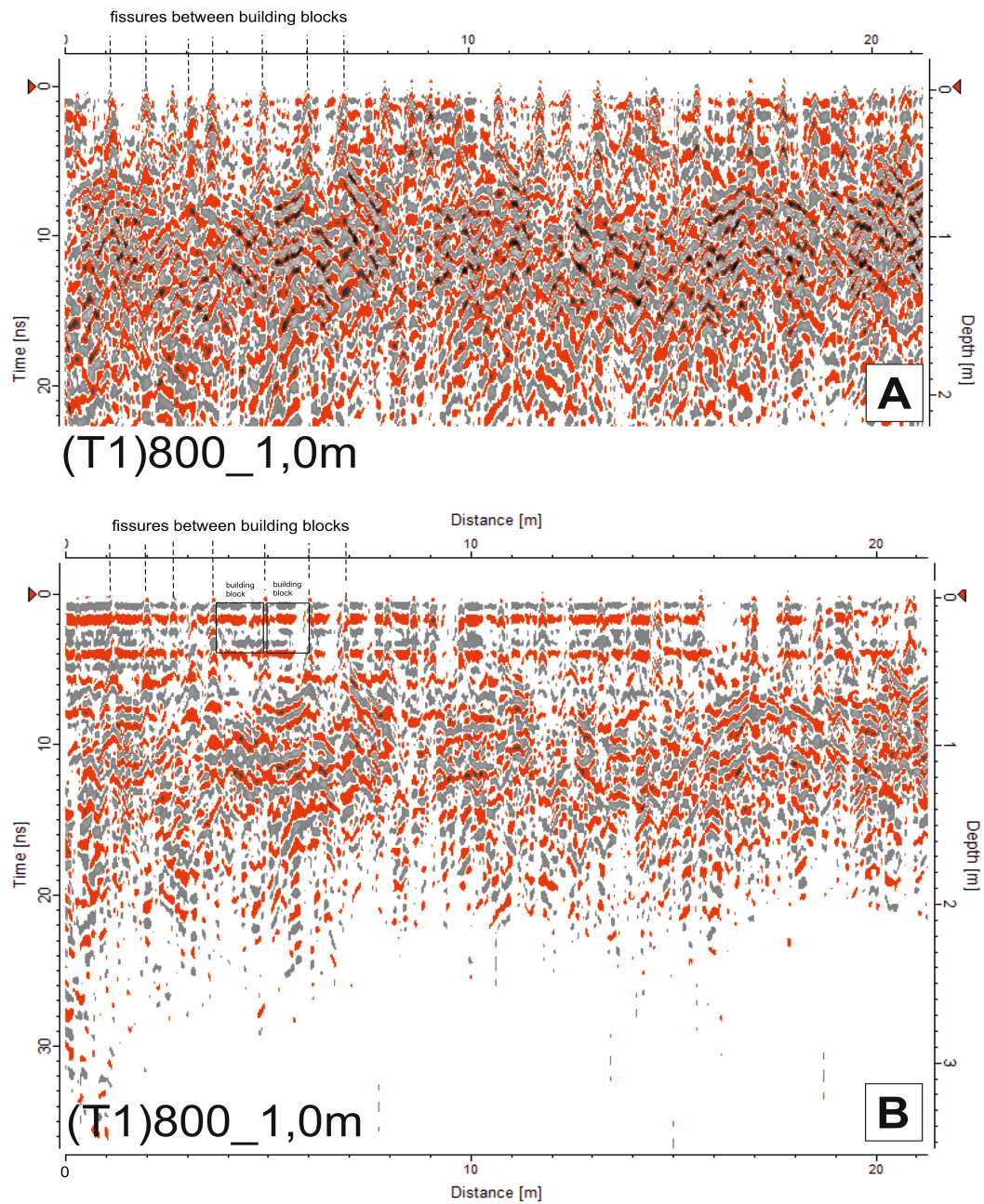


**FIG. 6** – Fragment of a processed GPR cross-section recorded with 800 MHz antennas. Radargram A: the gaps between the housing blocks can be noticed; Radargram B: the blocks of the tunnel casing can be observed.



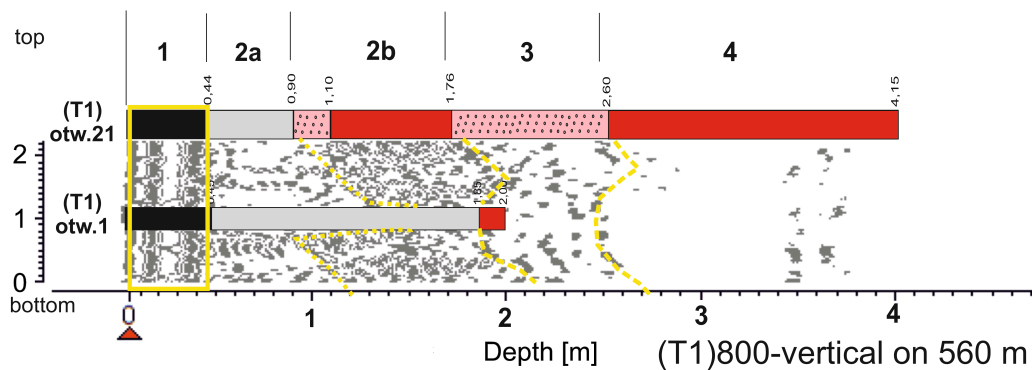


**FIG. 7** – Depth-scale calibration and interpretation of GPR data, by exploiting two geological horizontal drillings in the northern wall of the tunnel, namely drillings (T1)otw.1 and (T1)otw.21. The GPR radargram is (T1)800MHz-vertical, at 560 m. The legend used for the lithology is the same as in Figure 1.

As expected, GPR cross-sections give information about the ground structures until different depths, when antennas working at different frequencies are used. In particular, the 100 MHz antennas allow reaching a depth of about 21-60 m from the ground surface; the 250 MHz antennas provide information up to about 7-9 m from the tunnel wall; and, the 800 MHz antennas allow reaching a depth of about 4 m from the wall surface of the tunnel. On two-dimensional GPR cross-sections, the depth error has been estimated as follows: approximately  $\pm 1$  m with the 100 MHz antennas,  $\pm 0.5$  m with the 250 MHz antennas, and  $\pm 0.1$  m with the 800 MHz antennas. On the GPR sections, the cementation zone cannot be distinguished from the weathering; this is probably due to the almost 100-year impact of destructive processes on the structure of the tunnel and on the rocks surrounding the tunnel.

### 3. RESULTS

From GPR tests carried out on the surface of the terrain over the tunnel it follows that behind the tunnel casing there is a zone of debris and rubble reaching up to a depth of about 5 m; see Figures 9 and 10 (the rubble and debris region is indicated with 2 in Figure 10). Behind, there is a zone of crumbled (and possibly weathered) granite that reaches

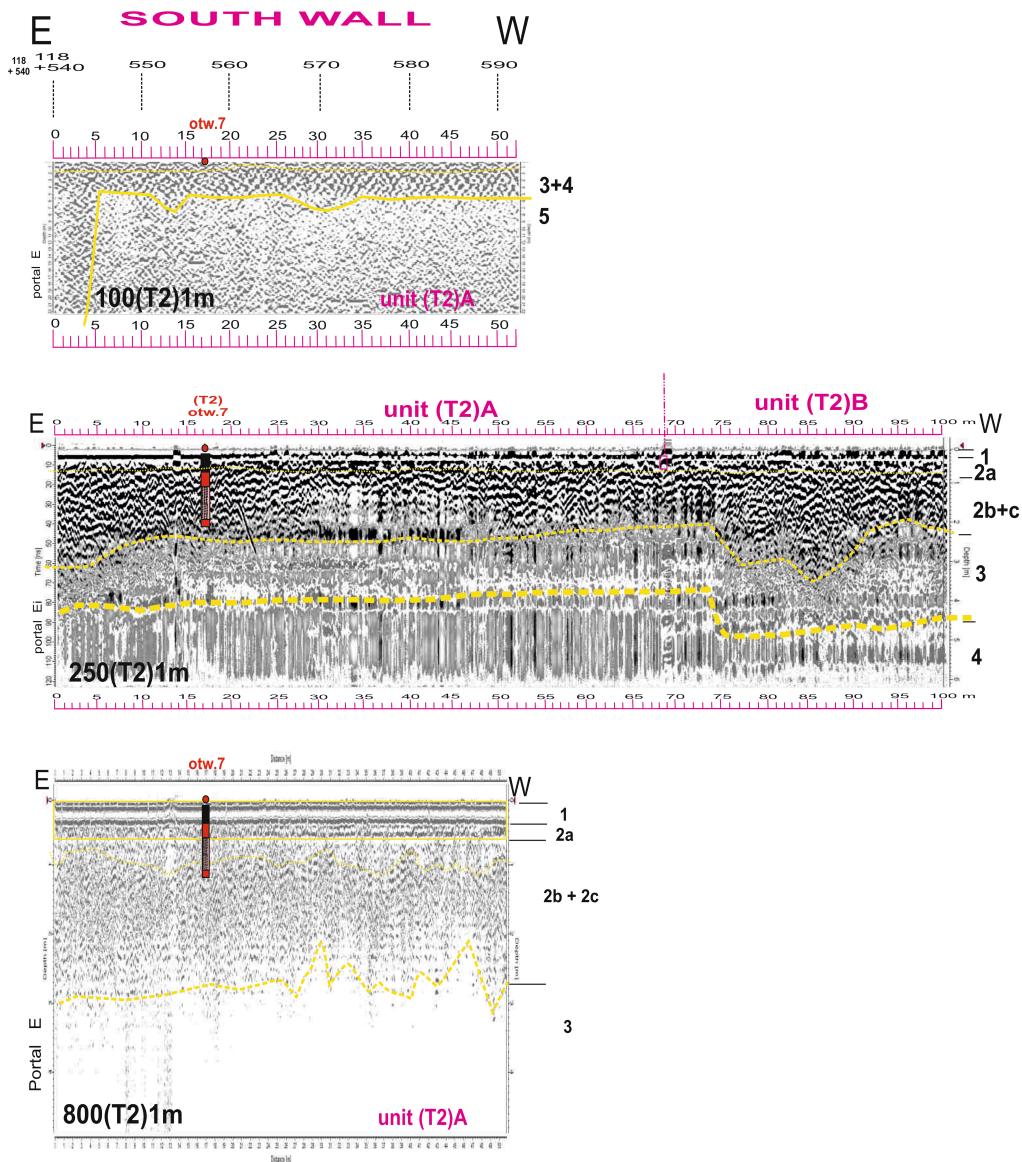


**FIG. 8** – Comparison of GPR data obtained with different antennas (100 MHz, 250 MHz, 800 MHz) over a fragment of the southern wall of the tunnel (unit (T2)A). Cross-sections obtained at 1 m height from the floor of the tunnel. The legend used for the lithology is the same as in Figure 1.

north and south up to about 15 m from the tunnel's axis (indicated with 3 in Figure 10). It was also pointed out that on all cross-sections (made over the tunnel) there are characteristic structures of ground subsidence (4 in Fig. 10).

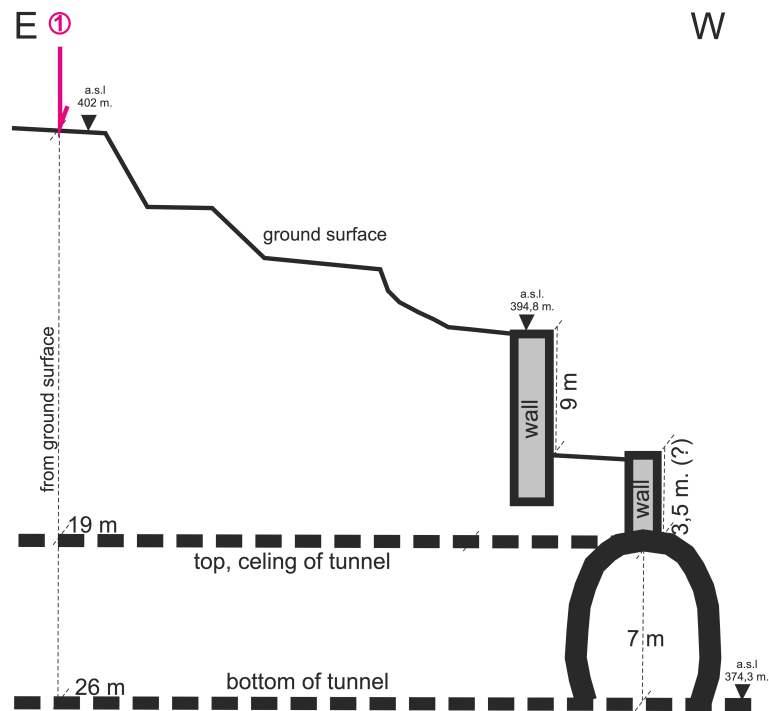


**FIG. 9** – Location of GPR cross-section No. 1 (100 MHz), above the tunnel.

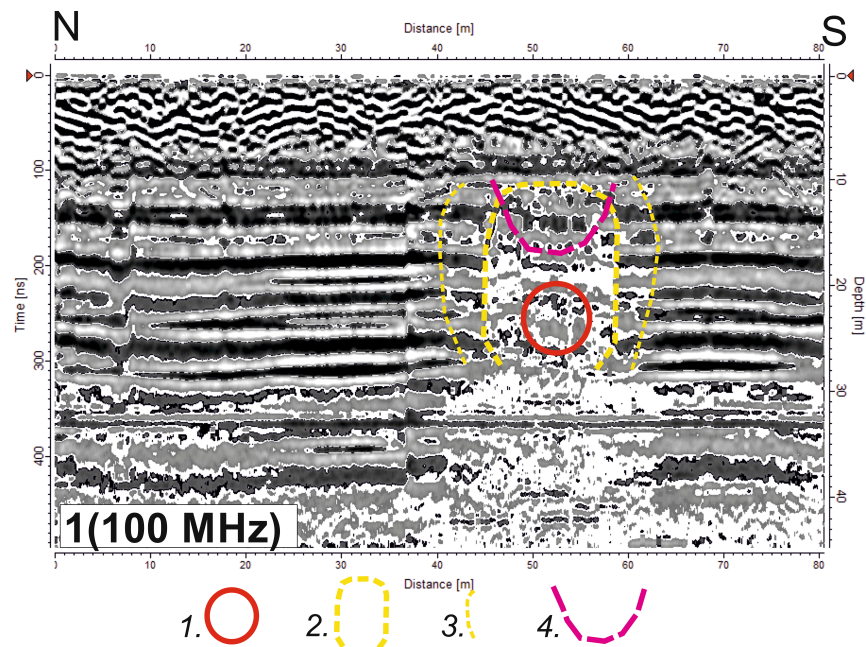


**FIG. 10** – GPR Cross-section No. 1 (100 MHz), above the tunnel. Geological interpretation: 1) Tunnel, 2) Destroyed rock mass, sprinkle, weathered rocks; 3) Granite strongly cracked, weathered; 4) Ground subsidence zone above the tunnel ceiling.

An exemplary fragment of a GPR cross-section recorded on the tunnel ceiling is presented in Figure 11 and clearly shows the condition of the ceiling. It is apparent that the housing blocks moved against each other, with a tendency to fall into the tunnel interior (1 in radargram A, in Figure 11). The cementing zone behind the casing in some places may be up to 1 m thick (2a in radargrams A and B, in Figure 11), and the rocks are crushed after it (2b in radargrams A and B, in Figure 11). The loss of housing blocks inside the tunnel is also confirmed by visual observations of the tunnel walls. In order to temporarily stop the movements of the housing blocks, suitable wooden wedges have been hammered into the interstices between the blocks (Figure 12).

Figures 13, 14 and 15 resume the results obtained by inspecting with GPR the north tunnel wall, at the T1 track and at a height of 1 m from the tunnel floor. In particular, results in Figure 13 were recorded by using the 100 MHz antennas; in Figure 14, results obtained with the 250 MHz antennas are presented; and, in Figure 15 results of investigations conducted with the 800 MHz antennas are shown.

The data obtained by using 100 MHz antennas allow to recognize only the boundaries between weathering and crumbling rocks (3/4 in Figure 13) and between crushed rocks and hard rocks (4/5 in Figure 13). This means that, with the help of 100 MHz antennas, the distance from the case to the hard rocks can be determined (5 in Figure 13) and the remaining boundaries are very poorly legible. These data do not provide information on the condition of the tunnel housing.

The results of the 250 MHz antenna tests allow to recognize only the boundary between weathered and weathered rocks (2/3 in Figure 14) and the boundary between weathered granites and strongly cracked rocks (3/4 in Figure 14). The cementation zone (2a in Figure 14) is barely visible, and the tunnel casing (1 in Figure 14) is poorly visible.

Finally, the data obtained by using the 800 MHz antennas clearly reveal the condition of the tunnel casing (1 in Figure 15), the cementing zone (2a in Figure 15), as well as the zone of weathered, gravel-sandy fillings (2b in Figure 15). The remaining boundaries are very poorly legible. A thorough analysis of data obtained from the 800 MHz antennas allows to visualize the gap widths in the tunnel casing (e.g., radargram A in Figure 6) and to illustrate the state of the tunnel casing blocks (e.g., radargram B in Figure 6).



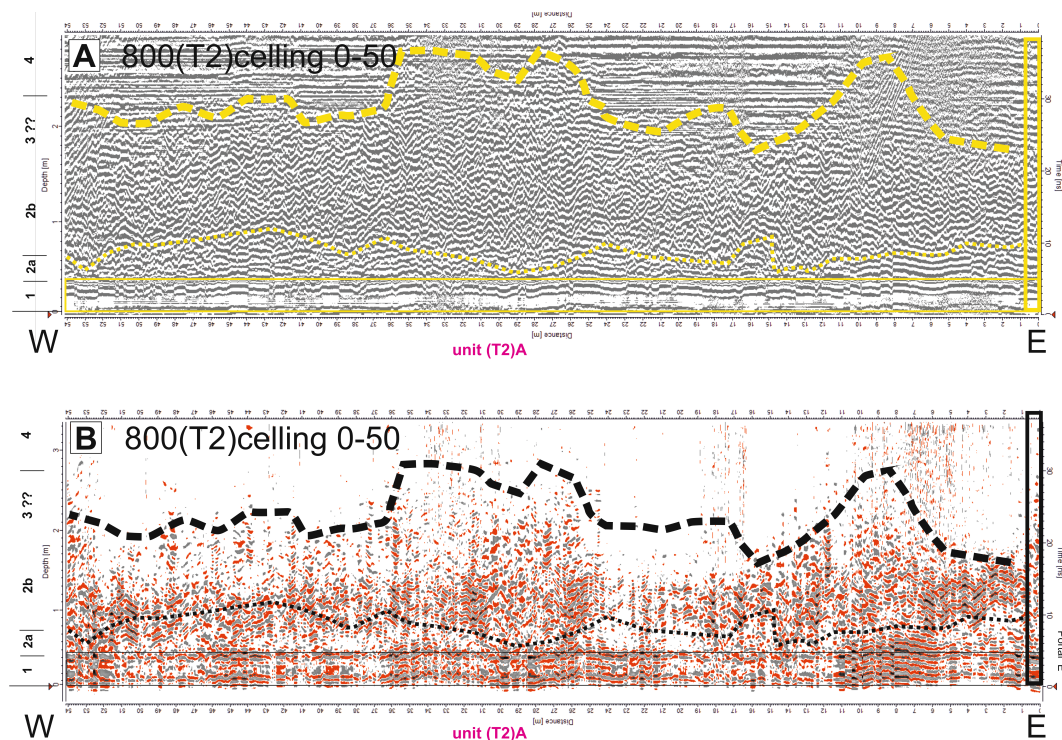


**FIG. 11** – The ceiling of the tunnel: interpretation of GPR data recorded with 800 MHz antennas. Lithology numbers are the same as in Figure 1.



**FIG. 12** – Photo of the tunnel ceiling, showing the falling blocks of the housing and the wooden wedges hammered into fissures between blocks to temporarily stop their movements.

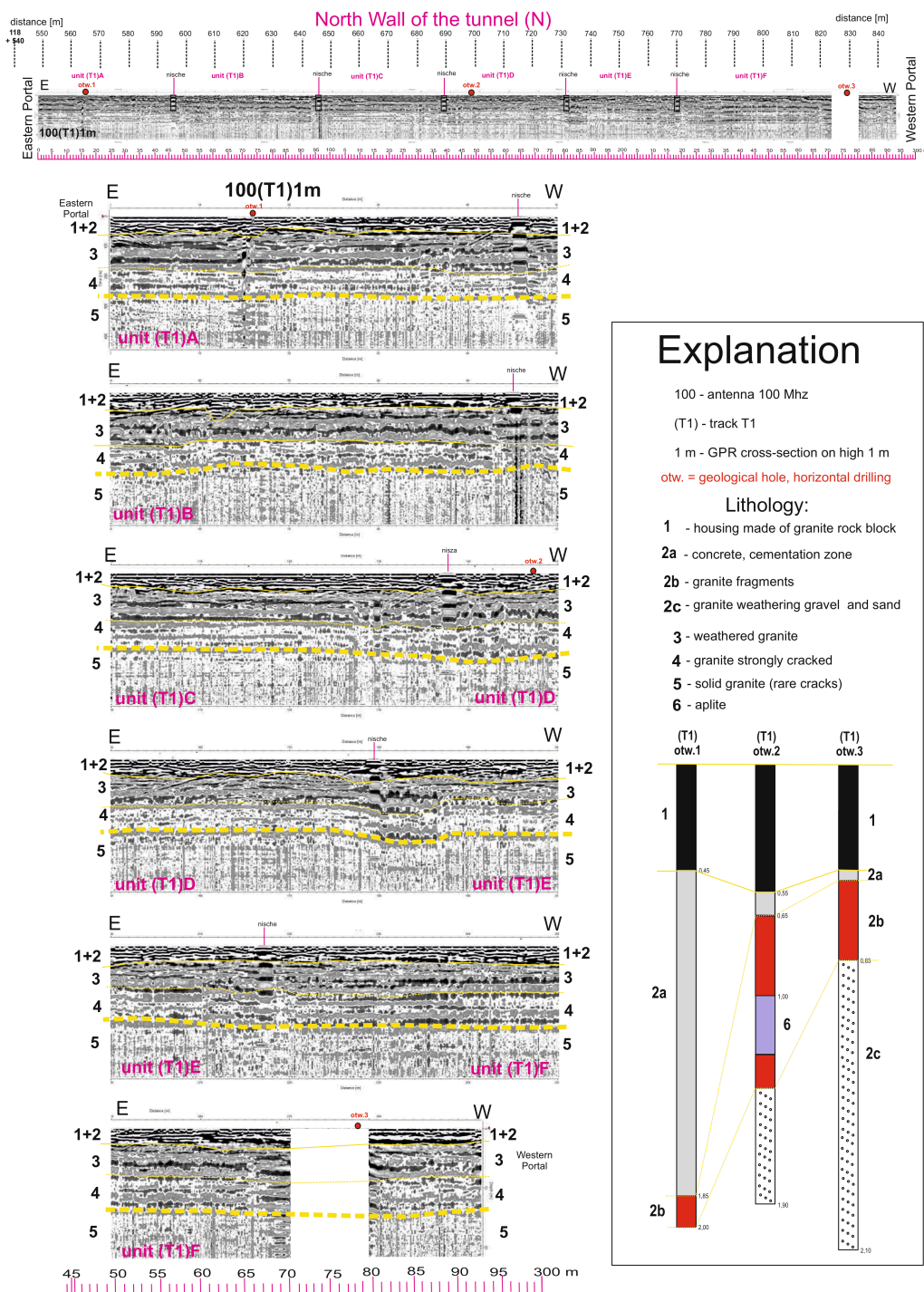


**FIG. 13** – GPR cross-section obtained with 100 MHz antennas along the northern wall of the tunnel, at the T1 track and at a height of 1 m from the tunnel floor.



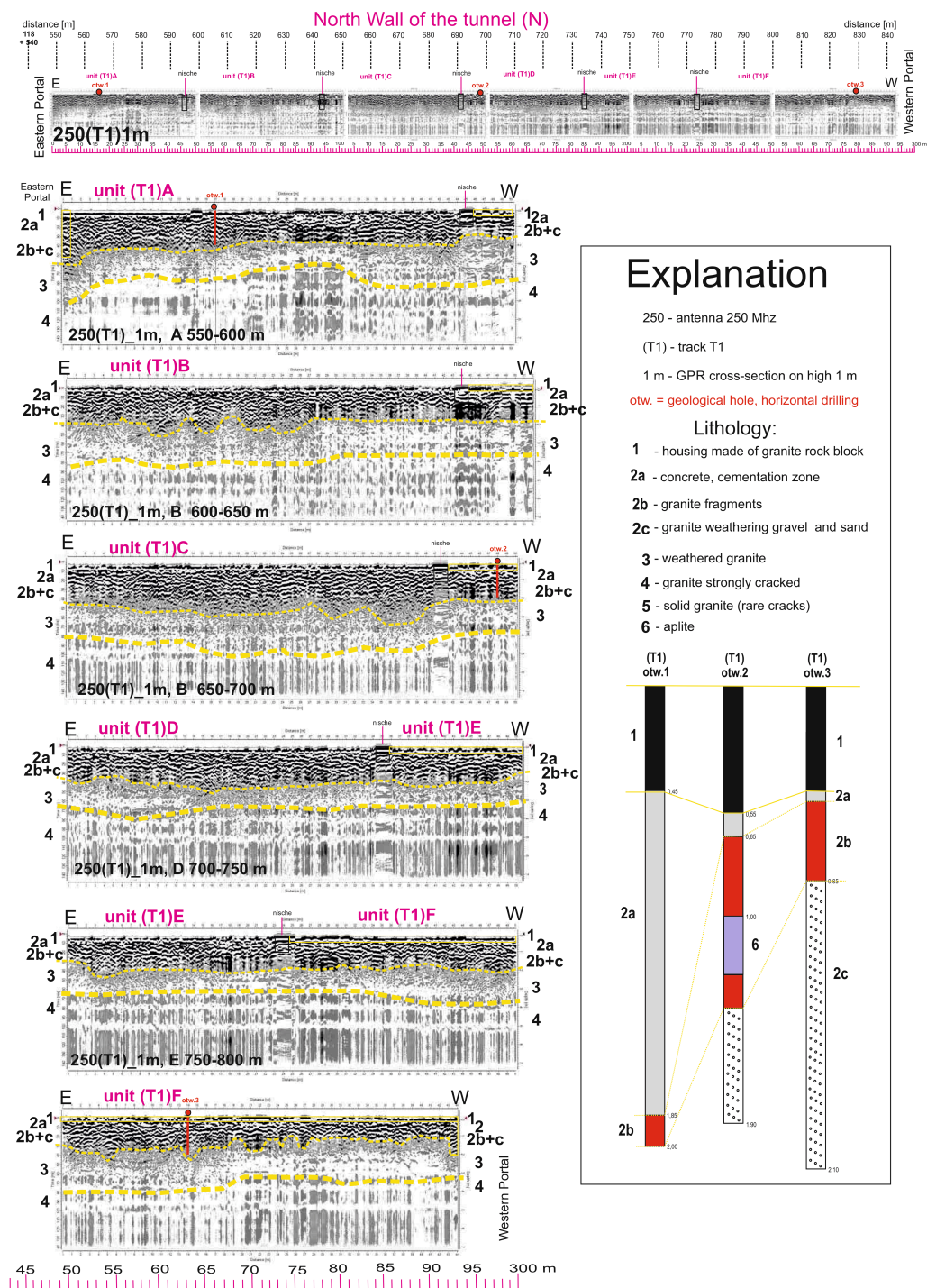


**FIG. 14** – GPR cross section obtained with 250 MHz antennas along the northern wall of the tunnel, at the T1 track and at a height of 1 m from the tunnel floor.



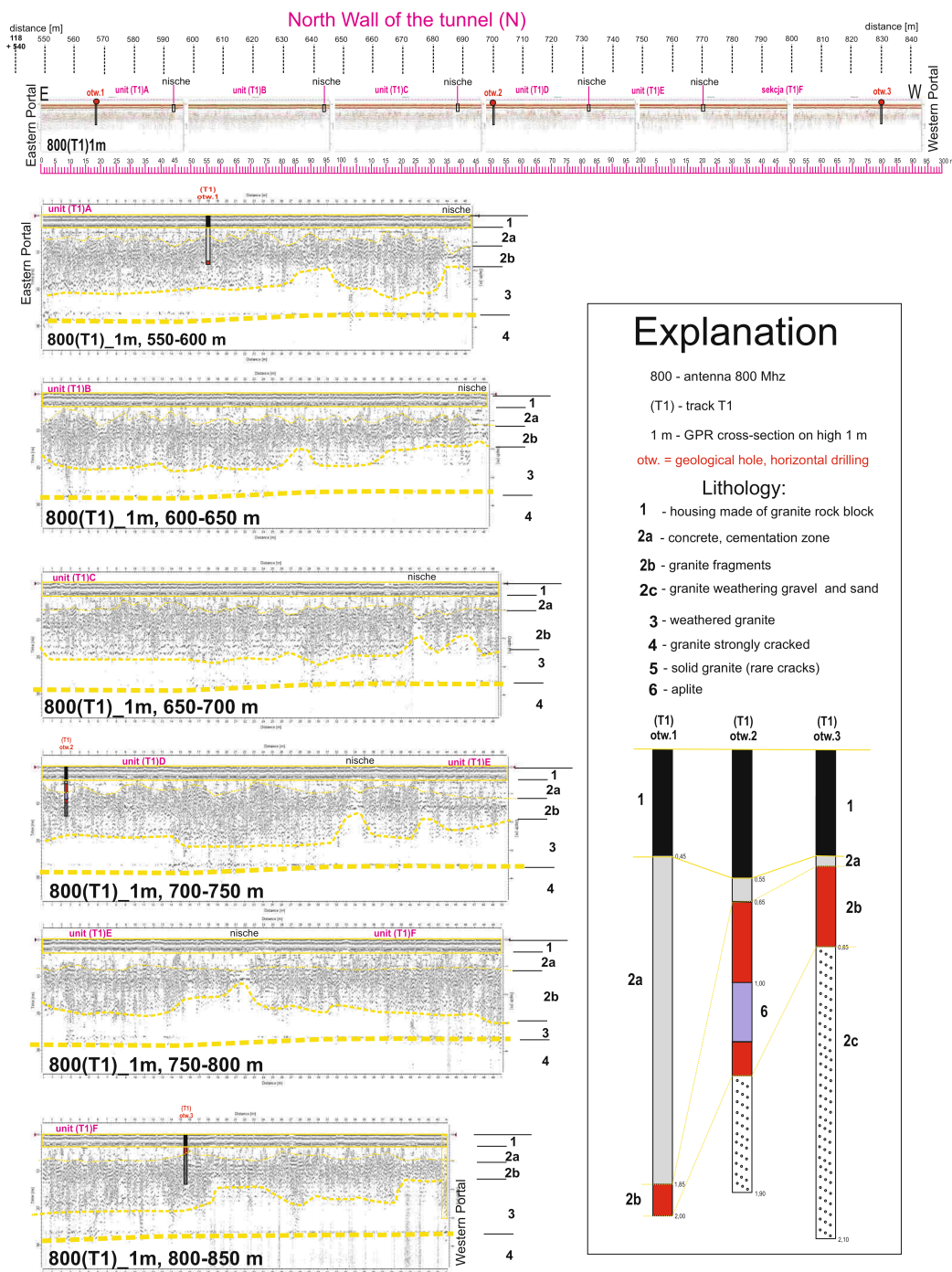


**FIG. 15** – GPR cross section obtained with 800 MHz antennas along the northern wall of the tunnel, at the T1 track and at a height of 1 m from the tunnel floor.

A preliminary analysis of GPR data in a three-dimensional system was done by Magdalena Udyrys (Sumo Services, Poland). This was just a “trial analysis” because, due to budget constraints, the ordering company of this GPR study accepted to pay for the execution of just a few lines along the walls of the tunnel. It would have been interesting to implement a three-dimensional analysis for some vertical sections of the tunnel, too (e.g., from the base of the walls to the axis of the tunnel ceiling, at intervals of 1 m).

By using the 800 MHz antennas, horizontal, parallel cross-sectional lines were recorded at a height of 1, 2, and 3.5 m from the tunnel floor on wall N, as well as at a height of 1, 2, 3.5, and 5 m from the tunnel floor on wall S. Based on these data, an analysis in a three-dimensional system was performed; unfortunately, while maintaining the same scales (horizontal and vertical), the obtained drawings turned out to be too long and with low height (so they are poorly legible).

To illustrate the results of the analysis, examples are presented in Figures 16 and 17, for the southern and northern walls of the tunnel, respectively. In the figures, sections and locations of bores made in the tunnel walls have been marked. On shallow time slices (e.g., from 0-0.15 m) niches in the tunnel walls can be clearly noticed (red points). On these “horizontal” time slices, warm colors (red, orange, yellow) correspond to anomalous spots indicating loosening in the tunnel casing or behind the tunnel casing.

In particular, let us examine more in detail Figure 16, recorded on the southern wall of the tunnel along T2: three examples of time cuts were chosen, corresponding to depths of 0-0.05 m, 2.49-2.54 m, and 3.28-3.33 m. Very poor condition of the housing (red, orange, yellow hues) can be observed on the tunnel section 0-56 m (time slice at a depth of 2.49-2.54 m) as well as on the tunnel section 2.40-2.95 m (time slice at a depth of 3.28-3.33 m), i.e., near the eastern and western tunnel portal.

Let us now examine more in detail Figure 17, recorded on the northern wall of the tunnel along track T1. In this case, very poor condition of the housing is on the tunnel section 0.8-2.15 m (time slice for a depth of 0.2-0.5 m). The worst situation is observed on the tunnel section 1.2-1.75 m (cut at a depth of 0.2-0.44 m).

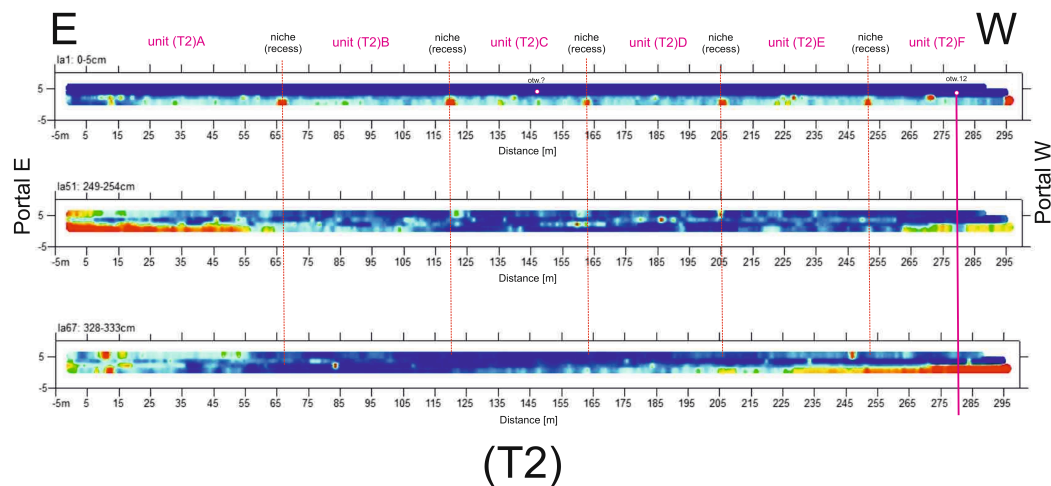


**FIG. 16** – Southern wall of the tunnel, T2 track. Selected time slices.

For what concerns the bottom of the tunnel, GPR cross-sections made in the tunnel along the railway tracks indicate that the sleepers under the rails lie on a subgrade build with crushed rock. Below, there is no concrete reinforcement (e.g., concrete slabs): the subgrade lies directly on a granite weathered cover or on cracked rock. Under the tracks, the covers of weathering, including the cracked rocks lying under them, extend until a depth of about 3-3.5 m. Below there are fractured granites in which fault zones have been found. These results are illustrated in Figure 18.

#### 4. CONCLUSIONS

GPR tests in the area of Wojanów railway tunnel were made, with antennas having the following central frequencies: 100 MHz, 250 MHz, and 800 MHz. The linear profiling method was used and data were represented in a two-dimensional system.

GPR profiling was carried out: above the tunnel, near the west portal; along the ceiling of the tunnel; along the northern wall of the tunnel (1, 2, and 3.5 m above the tunnel's base); along the southern wall of the tunnel (1, 2, 3.5, and 5 m above the tunnel's base); all along the tunnel floor, on the two tracks, as well as close to the tunnel walls.

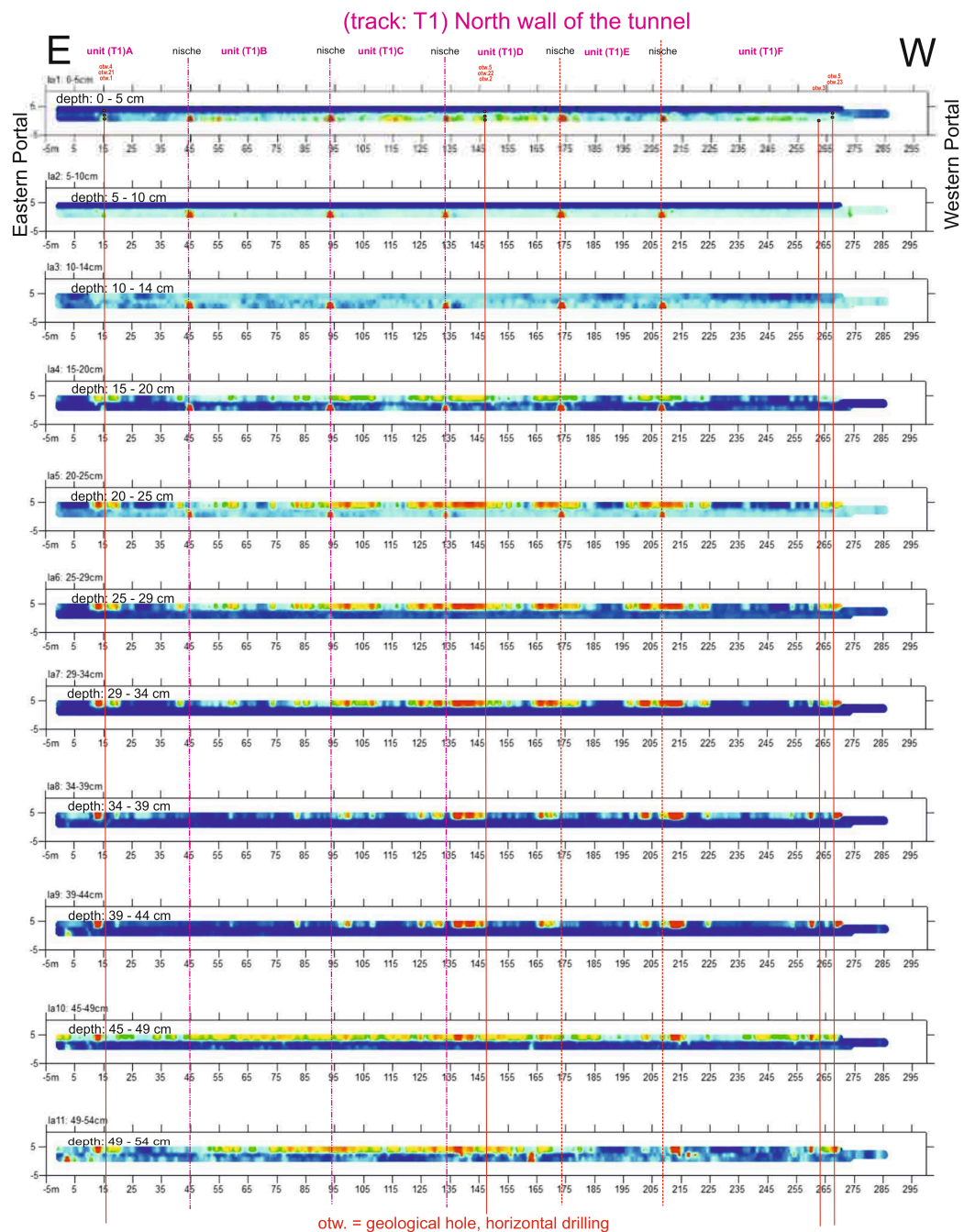


**FIG. 17** – Northern wall of the tunnel, T1 track. Selected time slices.



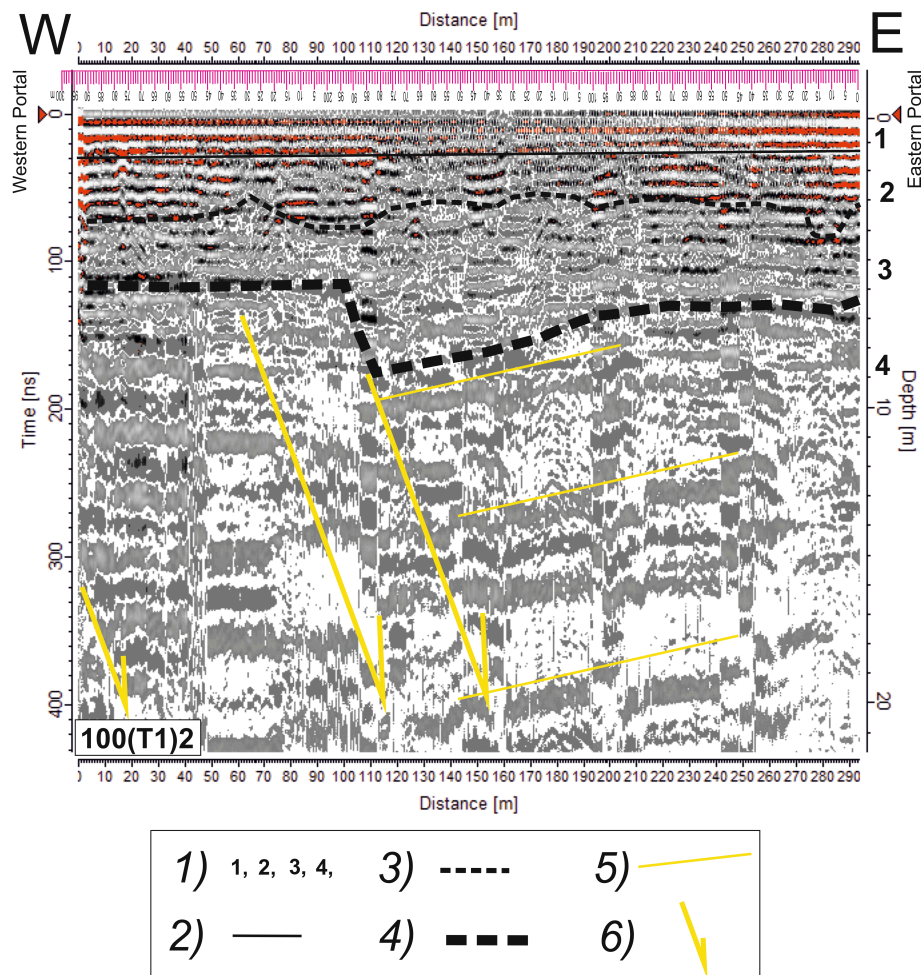


**FIG. 18** – Floor of the railway tunnel, subgrade of the track. Interpretation of GPR data (100 MHz antennas). Lithology: 1) 1 – track foundations and subgrade crushed rock; 2 – weathered rock; 3 – strongly fractured rocks; 4 – solid granite; 2) subgrade limit; 3) weathered rocks limit; 4) strongly fractured rocks limit; 5) boundaries of rock layers; 6) faults, dislocations.

Calibration of the depth scale on GPR cross-sections was made on the basis of data from 15 horizontal geotechnical drillings. The estimated depth error on the vertical scale is: 1 m with the 100 MHz antenna, 0.5 m with the 250 MHz antenna, and 0.1 m with the 800 MHz antenna. The obtained GPR cross-sections give information about the ground structure down to the following depths: about 21-60 m from the ground surface with the 100 MHz antenna, approximately 7-9 m

from the tunnel area/wall with the 250 MHz antenna, and about 4 m from the wall surface of the tunnel with the 800 MHz antenna.

On GPR cross-sections the following lithological assemblies can be distinguished and the forecasted boundaries between them are shown: 1) housing/granite blocks; 2a) concrete, cementation zone; 2b) granite debris (gravel) + granite fragments; 2c) gravel, sand; 3) weathered granite; 4) granite strongly cracked; 5) solid granite (rare cracks). On some cross-sections the systems of cracks in granite and possible faults can be observed. These structures have an inclination towards south.

The analysis of GPR data obtained with the 100 MHz antenna shows that behind the casing there is a zone of debris and rubble reaching down to a depth of about 5 m.

The analysis of GPR data obtained with the 250 MHz antennas shows that behind the housing there is a zone of cementation and weathering reaching down to a depth of about 2-4 m, behind such zone there is a crumbled zone of granite rocks (weathered?), which goes to a depth of 4-5 m from the surface of the tunnel casing.

The cross-sections obtained with the 800 MHz antenna show the condition of the tunnel casing (extended blocks, gap between the blocks, thickness of the housing blocks). However, a careful analysis of these data was not the goal of the research. To answer the question what is the condition of the housing, it would be necessary to enlarge the cross-sections and describe each block of housing separately.

The analysis of GPR data recorded with the 800 MHz antenna also shows that the housing blocks have variable thickness (up to 0.55 m). Behind the housing there is a variable thickness of the cementing zone. The cementing zone can reach a depth of 1.1 m (locally up to 2 m). Behind the casing there is a zone of debris and rock rubble reaching down to a depth of about 4 m (counting from the surface of the casing).

A preliminary analysis of GPR data in a three-dimensional system highlights a very poor condition of the housing and the zone behind the housing close to the western portal and near to the eastern portal (along sections of about 50 m).

For the anomalous zones detected in the two-dimensional system, it would be useful – as a future study – to perform a GPR survey on a

fine grid and analyze data in a three-dimensional system (parallel cross-sections could be collected every 1 m or, even better, every 0.5 m), from the tunnel floor to the ceiling axis of the tunnel.

For accurate GPR tests in tunnels, it is recommended to divide the tunnel under test into smaller parts (units) and analyze them separately.

## ACKNOWLEDGEMENTS

Thanks for financing and technical assistance during field tests to Wilhelm Janusz Szczurek (Biuro Inżynierskie Wrocław, Poland), Piotr Szczurek (Geostandard, Wrocław, Poland), Oktawia Ciapka (Politechnika Wrocławska, Wrocław, Poland), and to Magdalena Udyrysz (Sumo Services, Upton Severn, Worcestershire, England) for helping with the three-dimensional method.

## REFERENCES

- [1] A. Benedetto and L. Pajewski, Eds. "Civil Engineering Applications of Ground Penetrating Radar," Publishing House: Springer International; Book Series "Springer Transactions in Civil and Environmental Engineering;" April 2015; e-book ISBN: 9783319048130; hardcover ISBN: 9783319048123; doi: 10.1007/9783319048130; 371 pp.
- [2] W. Wai-Lok Lai, X. Dérobert, and P. Annan, "A review of Ground Penetrating Radar application in civil engineering: A 30-year journey from Locating and Testing to Imaging and Diagnosis," NDT & E International, vol. 96, pp. 58–78, June 2018, doi: 10.1016/j.ndteint.2017.04.002.
- [3] O. Abraham and X. Dérobert, "Non-destructive testing of fired tunnel walls: the Mont-Blanc Tunnel case study," NDT & E International, vol. 36, pp. 411–418, September 2003, doi: 10.1016/S0963-8695(03)00034-3.
- [4] E. Cardarelli, C. Marrone, and L. Orlando, "Evaluation of tunnel stability using integrated geophysical methods," Journal of Applied Geophysics, vol. 52, pp. 93–102, February 2003, doi: 10.1016/S0926-9851(02)00242-2
- [5] A. G. Davis, M. K. Lim, and C. G. Petersen, "Rapid and economical evaluation of concrete tunnel linings with impulse response and impulse radar non-destructive methods," NDT & E International, vol. 38, no. 3, pp. 181–186, April 2005, doi: 10.1016/j.ndteint.2004.03.011.
- [6] G. Parkinson and C. Ekes, "Ground penetrating radar evaluation of concrete tunnel linings," Proceedings of the 12th International Conference on



Ground Penetrating Radar (GPR 2008), 16–19 June 2008, Birmingham, United Kingdom, 2008.

[7] F. Lehmann, “Practical application of non-destructive test methods at a single-shell tunnel lining,” Proceedings of the 7th fib PhD Symposium, Stuttgart, Germany, 11–13 September 2008, published on the December 2008 issue of the e-Journal of Nondestructive Testing, pp. 1-10.

[8] A. Laluge and I. Hoff, “Determination of space behind precast concrete elements in tunnels using GPR,” Proceedings of the 13<sup>th</sup> International Conference on Ground Penetrating Radar (GPR 2010), 21–25 June 2010, Lecce, Italy, doi: 10.1109/ICGPR.2010.5550195.

[9] F. Zhanga, X. Xie, and H. Huang, “Application of ground penetrating radar in grouting evaluation for shield tunnel construction,” Tunnelling and Underground Space Technology, vol. 25, pp. 99-107, March 2010, doi: 10.1016/j.tust.2009.09.006.

[10] M.-J. Li, Y.-G. Zhao, H. Liu, Z. Wan, J.-C. Xu, X.-P. Xu, Y. Chen, and W. Bin, “Layer recognition and thickness evaluation of tunnel lining based on ground penetrating radar measurements,” Journal of Applied Geophysics, vol. 73, no. 1, pp. 45–48, January 2011, doi: 10.1016/j.jappgeo.2010.11.004.

[11] J. Karlovsek, A. Schuerann, and D. J. Williams, “Investigation of voids and cavities in bored tunnels using GPR,” Proc. 14th International Conference on Ground Penetrating Radar (GPR 2012), 4–8 June 2012, Shanghai, China, pp. 496–501, doi: 10.1109/ICGPR.2012.6254916.

[12] H.-Z. Yu, Y.-F. Ouyang, and H. Chen, “Application of Ground Penetrating Radar to Inspect the Metro Tunnel,” Proc. 14th International Conference on Ground Penetrating Radar (GPR 2012), 4–8 June 2012, Shanghai, China, pp. 759–763, doi: 10.1109/ICGPR.2012.6254963.

[13] X. Xie and C. Zeng, “Non-destructive evaluation of shield tunnel condition using GPR and 3D laser scanning,” Proceedings of the 14th International Conference on Ground Penetrating Radar (GPR 2012), 4–8 June 2012, Shanghai, China, pp. 479–484, doi: 10.1109/ICGPR.2012.6254913.

[14] X. Xiong, Q. Zhou, T. Zhou, Y. Ma, and K. Wan, “Application of GPR Technique and Research on High-speed Railway Tunnel,” Proceedings of the 14th International Conference on Ground Penetrating Radar (GPR 2012), 4–8 June 2012, Shanghai, China, pp. 524–529, doi: 10.1109/ICGPR.2012.6254920.

[15] Y. Hai-zhong, O. Yu-feng, and C. Hong, “Application of Ground Penetrating Radar to Inspect the Metro Tunnel,” Proceedings of the 14th International Conference on Ground Penetrating Radar (GPR 2012), 4–8 June 2012, Shanghai, China, pp. 759–763, doi: 10.1109/ICGPR.2012.6254963.

- [16] L. Xiang, H.-L. Zhou, Z. Shu, S.-H. Tan, G.-Q. Liang, and J. Zhu, "GPR evaluation of the Damaoshan highway tunnel: a case study," *NDT & E International*, vol. 59, pp. 68–76, October 2013, doi: 10.1016/j.ndteint.2013.05.004.
- [17] Q. Cun-chang, Z. Hui-lin, Y. Qi-ming, and Y. Xu, "Automatic detection of the grout layer of metro tunnel by GPR," *Applied Mechanics and Materials*, vol. 556–562, pp. 2719–2722, May 2014, doi: 10.4028/www.scientific.net/AMM.556-562.2719.
- [18] A.M. Alani and K. Banks, "Applications of ground penetrating radar in Medway Tunnel – inspection of structural joints," *Proceedings of the 15th International Conference on Ground Penetrating Radar (GPR 2014)*, Brussels, Belgium, 30 June – 4 July 2014, pp. 461–464, doi: 10.1109/ICGPR.2014.6970466.
- [19] X. Núñez-Nieto, M. Solla, F. J. Prego, and H. Lorenzo, "Assessing the applicability of GPR method for tunnelling inspection: Characterization and volumetric reconstruction," *Proceedings of the 8th International Workshop on Advanced Ground Penetrating Radar (IWAGPR 2015)*, Florence, Italy, 7–10 July 2015, pp. 1–4, doi: 10.1109/IWAGPR.2015.7292633.
- [20] J. White, S. Hurlebaus, P. Shokouhi, and A. Wimsatt, "Nondestructive Testing Methods for Underwater Tunnel Linings: Practical application at Chesapeake channel tunnel," *Proceedings of the 2015 International Symposium on Non-Destructive Testing in Civil Engineering*, Berlin, Germany, 15–17 September 2015, pp. 1–4.
- [21] Q.-M. Yu, H.-L. Zhou, Y.-H. Wang, and R.-X. Duan, "Quality monitoring of metro grouting behind segment using ground penetrating radar," *Construction and Building Materials*, vol. 110, pp. 189–200, May 2016, doi: 10.1016/j.conbuildmat.2015.12.109.
- [22] A. Lalague, M. Lebens, I. Hoff, E. Grov, "Detection of Rockfall on a Tunnel Concrete Lining with Ground-Penetrating Radar (GPR)," *Rock Mechanics and Rock Engineering*, vol 49, pp. 2811–2823, July 2016, doi: 10.1007/s00603-016-0943-y.
- [23] A. M. Alani and F. Tosti, "GPR applications in structural detailing of a major tunnel using different frequency antenna systems," *Construction and Building Materials*, vol. 158, pp. 1111–1122, January 2018, doi: 10.1016/j.conbuildmat.2017.09.100.
- [24] S. Cwojdzński and W. Kozdrój, "Detailed Geological Map of Poland on a scale of 1:50000, sheets Wojcieszów," [In Polish] "Szczegółowa Mapa Geologiczna Polski w skali 1:50000, ark. Wojcieszów," Państwowy Instytut Geologiczny - PIB, Warszawa, Poland, 2006.

- [25] M. Mierzejewski, "Decision regarding damage to a linear tunnel at km 118.548–118.841 railway line Wrocław-Jelenia Góra," [In Polish] "Orzeczenie w sprawie uszkodzeń tunelu liniowego w km 118.548–118.841 linii kolejowej Wrocław-Jelenia Góra," in: A. Solecki and W. Śliwiński, "Results of geophysical profiling using the EM31 apparatus in the tunnel on the Wrocław-Jelenia Góra route," [In Polish] "Wyniki profilowania geofizycznego przy użyciu aparatu EM31 w tunelu na trasie Wrocław-Jelenia Góra," Instytut Nauk Geologicznych Uniwersytetu Wrocławskiego Pracownia Usług Geologicznych "WRO-MIN," Wrocław, Dec. 1995, pp. 4 + 2 Figs.
- [26] M. Szalamacha and K. Tucholska, "Detailed Geological Map of the Sudetes in the scale of 1:25000, Jelenia Góra East sheet," [In Polish] "Szczegółowa Mapa Geologiczna Sudetów w skali 1:25000. Ark. Jelenia Góra Wschód," Wydawnictwo Geologiczne, Warszawa, 1957.
- [27] S. Staśko and R. Tarka, "Supply and drainage of groundwater in mountain areas on the basis of research in the Śnieżnik massif," [In Polish] "Zasilanie i drenaż wód podziemnych w obszarach górskich na podstawie badań w masywie Śnieżnika," Acta Universitatis Wrat., Prace Geologiczne-Mineralogiczne, 2528, pp. 1–86, Uniwersytet Wrocławski, 2002.

The scientific paper that you have downloaded is included in Issue 2, Volume 1 (July 2018) of the journal *Ground Penetrating Radar* (ISSN 2533-3100; journal homepage: [www.gpradar.eu/journal](http://www.gpradar.eu/journal)).

All *Ground Penetrating Radar* papers are processed and published in true open access, free to both Authors and Readers, thanks to the generous support of TU1208 GPR Association and to the voluntary efforts of the journal Editorial Board. The publication of Issue 2, Volume 1 is also supported by Adapis Georadar Teknik Ab ([georadar.eu](http://georadar.eu)) and by IDS Georadar s.r.l. ([idsgeoradar.com](http://idsgeoradar.com)).

The present information sheet is obviously not part of the scientific paper.

